Focusing of Shear Shock Waves

Bruno Giammarinaro, David Espíndola, François Coulouvrat, Gianmarco
Pinton

Focusing of Shear Shock Waves

Bruno Giammarinaro, David Espíndola, François Coulouvrat, and Gianmarco Pinton

Focusing of shear shock waves

Bruno Giammarinaro[1], David Espíndola[2], François Coulouvrat[1], and Gianmarco Pinton[2*]

[1] *Sorbonne Université, Université Pierre et Marie Curie - Univ Paris 06, CNRS,*
UMR 7190, Institut Jean le Rond d'Alembert, 4 place Jussieu, Paris, F-75005 France and
[2] *Joint Department of Biomedical Engineering, University of North Carolina at Chapel Hill,*
109 Mason Farm Road, CB 7575, Chapel Hill, North Carolina 27514, USA and North Carolina State University,
4130 Engineering Building III, CB 7115, Raleigh, North Carolina 27695, USA
(Dated: December 11, 2017)

Focusing is a ubiquitous way to transform waves. Recently, a new type of shock wave has been observed experimentally with high frame rate ultrasound: shear shock waves in soft solids. These strongly nonlinear waves are characterized by a high Mach number because the shear wave velocity is much slower, by three orders of magnitude, than the longitudinal wave velocity. Furthermore these waves have a unique cubic nonlinearity which generates only odd harmonics. Unlike longitudinal waves for which only compressional shocks are possible, shear waves exhibit cubic nonlinearities which can generate positive and negative shocks. Here we present the first experimental observation of shear shock wave focusing, generated by the vertical motion of a solid cylinder section embedded in a soft gelatin-graphite phantom to induce linearly vertically polarized motion. Raw ultrasound data from high frame rate (7692 images/second) acquisitions in combination with algorithms that are tuned to detect small displacements ($\sim 1\mu$m) are used to generate quantitative movies of gel motion. The features of shear shock wave focusing are analyzed by comparing experimental observations with numerical simulations of a retarded time elastodynamic equation with cubic nonlinearities and empirical attenuation laws for soft solids.

I. INTRODUCTION

Focusing is a fundamental tool of wave physics and it is used for uncountable applications. There are numerous methods that focus acoustical waves and they include curved sources, mirrors, lenses, and more recently, phased arrays [1], time-reversal processes [2] or metamaterial networks [3, 4]. In conventional materials the minimum size of the focal spot is determined by the wavelength. As a consequence, shock waves, which are broadband and have a high frequency content, can be focused efficiently. One of the first applications of shock wave focusing is to lithotripsy, which is now used to treat 85% of patients with kidney stones [5]. Shock waves, such as those that generate outdoor noise, can also be undesirable. For instance the sonic boom from supersonic flight, is focused during transonic acceleration [6] thus severely limiting flight at supersonic speed over land. In linear wave theory focusing is described by catastrophe theory [7, 8]. The two simplest caustics are the fold caustic and the cusp caustic. They have universal local diffraction patterns given respectively by the Airy and the Pearcey functions. However, shock waves are inherently a nonlinear wave process. Even for weak shock waves, it has been shown that nonlinear effects play a fundamental role around the focus, especially in limiting the overall field amplitude [9]. This has been studied extensively especially for fold [10, 11] and cusp caustics [12], and for point focusing with applications to lithotripsy [13].

Compared to compressional waves, shear waves are relatively unstudied because until recently there were no experimental methods that were capable of direct observation. In fluids, for example, a detector, such as a hydrophone, can be displaced within the medium to characterize wave propagation at depth. In solids, on the other hand, detector motion is impossible without disrupting the medium. Optical techniques that measure displacement have low penetration depths in opaque materials and would only be suitable for surface waves. The first observation of shear shock waves was reported in 2003 and it relied on ultrasound, i.e. a compressional wave, to quantify shear wave motion in gelatin [14]. For quasi-incompressible media like soft biological tissues or their phantoms, the elastic compressible parameters ($\sim$ GPa) are 6 orders of magnitude greater than shear parameters ($\sim$ kPa). This results in a difference of 3 orders of magnitude between the shear wave speed ($c_T \sim 1$ m/s) and the compressional wave velocity ($c_L \sim 1500 m/s$). This difference in speed is what has allowed the development of high frame-rate ultrasonic techniques to generate images of the elastic properties of *in vivo* soft tissue [15, 16]. Moreover, the slow speed of the shear waves is advantageous to the investigation of shock waves because the nonlinear effects are proportional to the square of the Mach number, which itself is inversely proportional to c_T. Low values of c_T therefore yield high Mach numbers.

The objective of this article is to present the first experimental observation of shear shock wave focusing. In addition to being motivated by the fundamental physics of nonlinear waves, we hypothesize that shear shock waves may be responsible for certain types of traumatic brain injuries (TBI). In particular 40 to 50% of deaths from TBI are due to diffuse axonal injuries which occur deep inside the brain, away from area of the primary impact [17]. We have recently observed that shear shock waves are generated and subsequently propagate in the

brain under impact conditions that are quite general [18]. For example, a 35g impact, which is in the concussive range, propagates nonlinearly in the brain and develops into a thin, destructive 300g shock front. This highly localized increase in acceleration suggests that shear shock waves are a fundamental mechanism for traumatic injuries in the brain and in soft tissue.

Shear waves could be focused by the spherical skull geometry and in the focal region, where the shear amplitude is magnified, shock waves could form locally, generating injury. This hypothesis is supported by preliminary results which indicate that the order of magnitude of measured impact velocities ($\sim$ a few m/s or more) for brain trauma is comparable to the shear wave velocity and thus results in Mach numbers of order one. Understanding shear shock wave focusing could therefore provide insight on the biomechanical environment that generates TBI's.
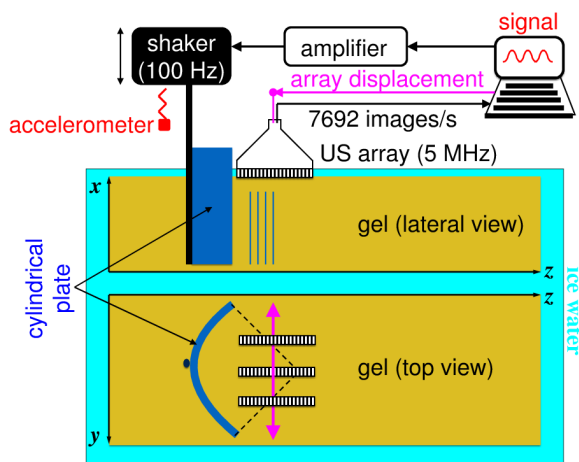
II. EXPERIMENTAL SETUP

Figure 1. Experimental set-up. A programmable high frame-rate ultrasound scanner measures shear motion generated by an electromechanical attached to a cylinder section embedded in gelatin.

The experimental setup (Fig.1) uses an electromechanical shaker attached to a cylinder section embedded in gelatin to generate shear waves. A programmable high frame-rate ultrasound scanner measures motion, . The water-based gelatin phantom, composed of 3.14% gelatin mimics the shear and compressional wave properties of soft tissue. Graphite powder was added with 1% concentration to provide acoustical scatterers that can be tracked with ultrasound. This gel phantom was poured into a 25 cm by 20 cm by 15 cm rectangular polypropylene container. The 90° arc of a PVC cylinder with a 7.5 cm radius of curvature and a height of 13 cm was placed in the gel (11 cm inserted vertically within the

gel). The gel was then allowed to set and cool in an ice-filled water tank. A constant 1°C temperature was maintained during the experiment to minimize changes in the mechanical properties. The electromechanical shaker connected to the cylinder section was used to drive motion in the vertical direction and generate the linearly polarized shear displacement.

A 5 cycle 100 Hz sinusoid enveloped by a Chebychev window was chosen as a driving signal. This signal has a -80 dB dropoff in the frequency domain which is required to separate the harmonics as they develop with nonlinear shear wave propagation. An accelerometer, attached to the cylinder section, indicated that the shaker motion was linear and that the harmonic generation occurs in the medium and is not generated by the source. There are currently no reports that directly measure the *in vivo* brain motion during traumatic events. However, estimates of skull or head motion, obtained with accelerometers indicate that the velocity for shear motion can be on the order of 1 m/s and acceleration can be on the order of several hundreds of m/s^2 [19]. We choose three levels of excitation for our experiment: weak (0.1 m/s), moderate (0.24 m/s) and strong (0.47 m/s) which have a Mach number ($M = v_0/c_T$) of 0.07, 0.17 and 0.33, respectively. Note that these Mach number are relatively high respect to the typical Mach number to produce acoustical shocks (10^{-2}) [20].

Gel motion was measured with a custom flash focus ultrasound sequence that we have previously developed for shock wave tracking using a programmable Verasonics Vantage scanner and a commercial Philips ATL L7-4 probe [18]. The imaging sequence consists of 16 focused transmit-receive events with an F-number of 4, synchronized with the shear wave generation. Each event has a constant 6 cm focal depth while the lateral position of the focus is shifted. In a post-processing stage, a conventional delay-and-sum beamforming is applied to generate, from each event, 1500 frames of 8 RF lines at a frame rate of 7692 images per second. All together, the 16 transmit-receive event produced a stack of beamformed ultrasonic RF images with 128 lines (4 cm width) each.

The harmonic development of the shock wave is challenging to measure due to the rapid motion of the gel and the high motion detection accuracy required to represent low-amplitude high frequency displacements. A dedicated shock displacement tracking algorithm that uses the raw ultrasound data was developed for this purpose [21]. It is optimized to track shock waves by using an adaptive quality-weighted median filter that maximizes the correlation coefficient in a way that accurately represents the sharp shock front. Note that in general, due to absorption, the shock front is not perfectly vertical, and it is characterized by a significant steepening of the waveform. Three-dimensional maps of gel motion were obtained by displacing the ultrasound array in the lateral y direction with a high precision ($10\mu m$) robotic arm. It was assumed that the source motion was uniform in the vertical direction x, and the measured speed data was av-
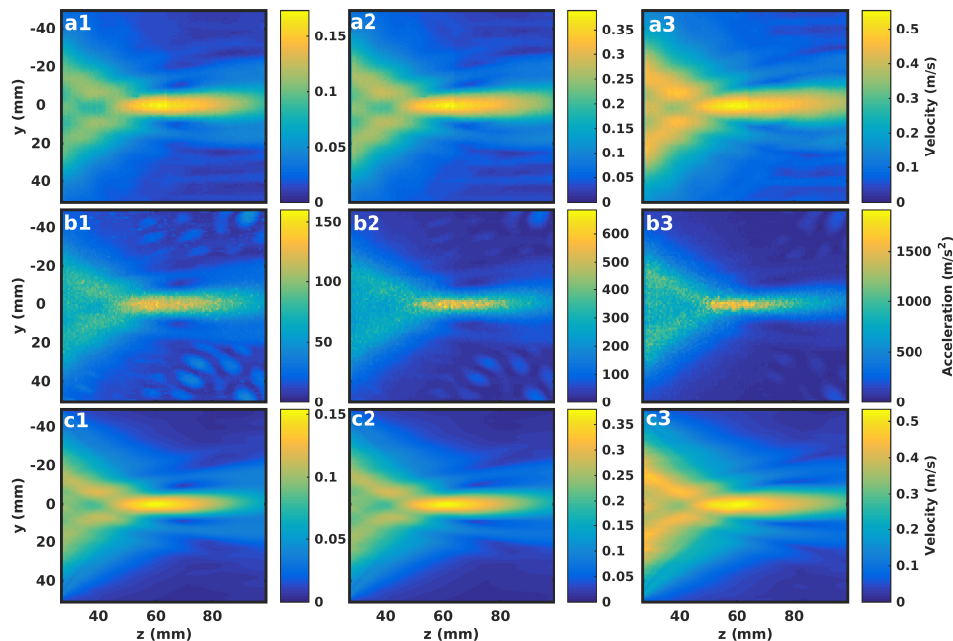
Figure 2. 2D (y, z) maps of the measured maximum velocity (ms^{-1}) (a) and maximum acceleration (ms^{-2}) (b) for shaker excitation amplitudes 0.1m/s(1), 0.24m/s(2) and 0.47m/s(3).

eraged over 100 measurement points (3 mm) vertically. The averaging was performed deep in the gel to remove unwanted boundary or surface effects. Thus, with the averaging the 3D data set was converted to 2D maps of shear displacement in the x direction as a function of y and z.

III. EXPERIMENTAL RESULTS

Examples of such 2D maps are shown in Fig. 2 for three shaker excitation levels, ranging from weakly (0.1m/s) to moderately (0.24m/s) to strongly (0.47m/s) non-linear. Row (a) shows the maximum velocity maps $max_t(v(y, z, t))$, row (b) shows the maximum acceleration $max_t(a(y, z, t))$ maps computed from the velocity maps with a time derivative based on the Fourier transform, and row (c) shows the maximum velocity maps computed from the simulation (described subsequently). To improve signal-to-noise ratio (SNR), frequencies above the 10th harmonic (1000 Hz) were not included in the derivative calculation because they are beyond the range of detectability for the ultrasound system. The figure outlines the shear wave focusing process. The size of focal spot, about 2 cm long and 1 cm wide, is in general agreement with expected laws of linear diffraction. Significant differences are visible between linear and nonlinear regimes. In the nonlinear cases, wave attenuation is enhanced relative to the linear case because of harmonic generation which shifts the frequency spectrum towards higher frequencies. This increased attenuation is more pronounced on the axis, where the amplitude is maxi-

mal, than off axis, which consequently tends to widen the focal spot (Fig. 2). Moreover, in the highly nonlinear case, due to the same process of energy being transferred within the spectrum, strong absorption occurs even before the focal spot, so that the focal gain is lower than in the linear case. Compared to the velocity, the focal spot for acceleration is narrower in width and shorter axially, i.e. it shrinks as a function of amplitude. This is due to the steepening of the wave-front from nonlinear propagation that tends to localize high acceleration [18, 22]. This is a highly nonlinear process because the input velocity spans a factor of five between the lowest and highest excitation. However, the velocity at the focus spans a factor of 3.7 and the acceleration spans a factor of approximately 12.

The shock steepening is clearly visible in Fig. 3 which plots the velocity (left) and the corresponding frequency spectrum (right) measured at $y = 0$, $z = 6$cm to illustrate this nonlinear process. To better visualize the time waveform, only the first four central periods of the maximum velocity are shown. The frequency spectra are normalized by the fundamental frequency at 100 Hz to outline the harmonic generation. There is a significant nonlinear wave distortion between weakly nonlinear shaker excitation (0.1 m/s, in 1) and the moderately (0.24 m/s, in 2) or strongly (0.47 m/s, in 3) nonlinear cases.

In the first, quasi-linear case, the waveform remains almost sinusoidal with a frequency spectrum centered at the transmitted 100 Hz frequency, with hardly any visible energy at the odd harmonics. For the intermediate case (0.24 m/s) the time waveform steepens, there is a significant amount of energy at the 3rd harmonic, and a
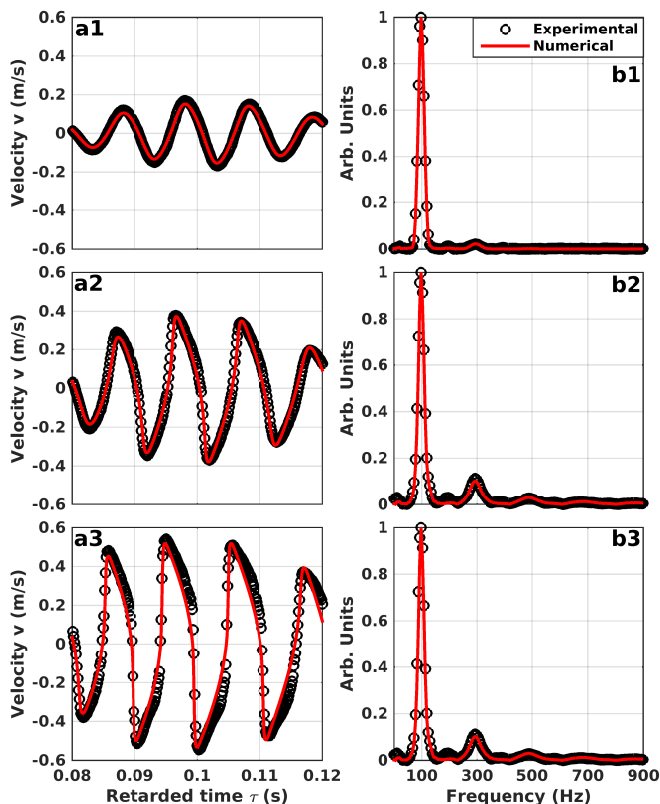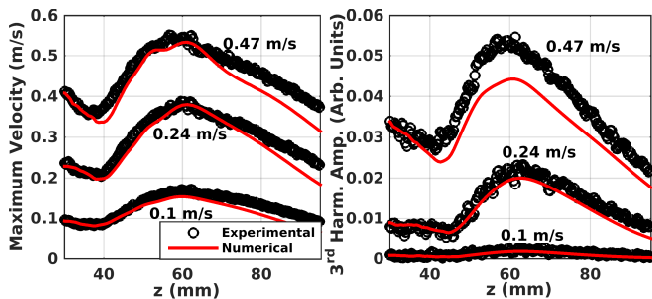
Figure 4. Measured and simulated maximum total velocity along the axis (left) and maximum velocity at the third harmonic frequency (right).

even in the strongest nonlinear case (0.47m/s) because the propagation distance is relatively short and focusing has not yet occurred. This measured field was then propagated numerically for different values of nonlinear cubic parameter β. A value of $\beta = 2.2 \pm 0.2$ yielded the best agreement between data and simulations along the axis as illustrated by Fig. (3) for the velocity time waveform (zoomed in on the four central periods) at the focal position ($y = 0, z = 6cm$). For the low amplitude case, the nonlinear effects are negligible, the waveform is almost sinusoidal and as expected the numerical simulations are insensitive to β. For the two other cases, there is a large nonlinear distortion leading to waveform steepening (0.24m/s) and shock wave formation (0.47m/s). The selected value $\beta = 2.2 \pm 0.2$ provides a very good agreement in both cases, thus indicating that the wave evolution is clearly dominated by cubic nonlinearities. Note that in Fig. 3, b3 there are some spectral fluctuations in the measured results that are subsequently propagated by the simulations. This may be an indirect consequence of the large driving amplitudes which may arise from surface waves, or deviation from the initial assumption of a purely polarized shear waves geometry. However accelerometric measurements indicate that the initial condition generated by the shaker were in fact linear.

The maximum velocity maps calculated by these simulations (Fig. 2 row (c)) show excellent agreement with experiments (Fig. 2 row (a)).

The measured and simulated maximum total velocity along the axis and the maximum velocity at the third harmonic frequency (Fig 4) are also in close agreement. Slight differences in the third harmonic in the strong nonlinear case (0.47m/s) may reflect the limits of theory that

is formally valid only for small Mach number, whereas in this case the Mach number reaches 0.38 at the focus. The total axial velocity has a focal spot near 58 mm with a weak dependence of this spot on the amplitude. However, for the third harmonic velocity, the focal distance depends more strongly on the driving amplitude, decreasing as the amplitude increases. This focal length shortening is analogous to the same classical observation in nonlinear acoustics [30].

V. DISCUSSION AND CONCLUSION

Previous reports of shear shock waves for a planar source show that the peak third harmonic amplitude occurs between a distance of 12.5 and 20.1 mm [14]. In the brain this third harmonic peak is between a distance of 5 and 7 mm [18]. Due to experimental constraints from the cylindrical geometry, the z-axis in Fig. 4 starts at 30 mm. For the large amplitude case (0.47m/s), between 30 and 42 mm, the third harmonic amplitude decreases, and then after 42 mm if starts increasing again as the shear wave converges to the focus. Nevertheless accelerometric measurements indicate that the third harmonic amplitude at $z = 0$ is negligible. We therefore hypothesize that there is a peak which not visible in the plots. Then, for the highly nonlinear case there is an initial rise in the third harmonic from near-field plane wave-like behavior then a decrease in the third harmonic from dissipation, followed by a second rise from focusing, and finally a second decrease from dissipation.

Thus, Fig. 4 indicates that three regimes, in terms of shock development, can be identified. First, at low amplitudes the attenuation dominates over nonlinearity and a shock is never formed. Second, at intermediate amplitudes the shock forms at the focus due to the increased amplitude from focusing and the rate of accumulation of nonlinear steepening with propagation. Finally, at high amplitudes, the shock forms before the the focal point and at the focus.

In summary this first experimental observation of shear shock wave focusing in a soft solid shows good agreement with nonlinear elastodynamic theory. Though performed *in vitro* with a biological phantom (gel), the present experiment scales realistically, in terms of geometry, amplitude and frequency, with the human skull and brain. These results suggest that the skull geometry could amplify high intensity mechanical effects deep inside the brain, and may play a significant role in traumatic brain injuries such as diffuse axonal injuries.

[1] S. Smith, G. Trahey, and O. von Ramm, "Phased array ultrasound imaging through planar tissue layers," Ultrasound in Medicine & Biology **12**, 229 – 243 (1986).

[2] M. Fink, "Time reversal of ultrasonic fields. i. basic principles," IEEE Transactions on Ultrasonics, Ferroelectrics, and Frequency Control **39**, 555–566 (1992).

[3] N. Fang, D. Xi, J. Xu, M. Ambati, W. Srituravanich, C. Sun, and X. Zhang, "Ultrasonic metamaterials with negative modulus," Nature materials **5**, 452–456 (2006).

[4] S. Zhang, L. Yin, and N. Fang, "Focusing ultrasound with an acoustic metamaterial network," Phys. Rev. Lett. **102**, 194301 (2009).

[5] C. Chaussy, W. Brendel, and E. Schmiedt, "Extracorporeally induced destruction of kidney stones by shock waves," The Lancet **316**, 1265 – 1268 (1980), originally published as Volume 2, Issue 8207.

[6] R. Blumrich, F. Coulouvrat, and D. Heimann, "Variability of focused sonic booms from accelerating supersonic aircraft in consideration of meteorological effects," The Journal of the Acoustical Society of America **118**, 696–706 (2005), https://doi.org/10.1121/1.1938547.

[7] R. Thom, "Structural stability and morphogenesis, 1975," Trans. by D. Fowler. Reading, Mass.: Benjamin (1975).

[8] M. Berry, "Waves and thom's theorem," Advances in Physics **25**, 1–26 (1976), https://doi.org/10.1080/00018737600101342.

[9] B. Sturtevant and V. A. Kulkarny, "The focusing of weak shock waves," Journal of Fluid Mechanics **73**, 651671 (1976).

[10] R. Marchiano, F. Coulouvrat, and R. Grenon, "Numerical simulation of shock wave focusing at fold caustics, with application to sonic boom," The Journal of the Acoustical Society of America **114**, 1758–1771 (2003), https://doi.org/10.1121/1.1610459.

[11] R. Marchiano, J.-L. Thomas, and F. Coulouvrat, "Experimental simulation of supersonic superboom in a water tank: Nonlinear focusing of weak shock waves at a fold caustic," Phys. Rev. Lett. **91**, 184301 (2003).

[12] R. Marchiano, F. Coulouvrat, and J.-L. Thomas, "Nonlinear focusing of acoustic shock waves at a caustic cusp," The Journal of the Acoustical Society of America **117**, 566–577 (2005), https://doi.org/10.1121/1.1841551.

[13] M. A. Averkiou and M. F. Hamilton, "Nonlinear distortion of short pulses radiated by plane and focused circular pistons," The Journal of the Acoustical Society of America **102**, 2539–2548 (1997), https://doi.org/10.1121/1.420308.

[14] S. Catheline, J.-L. Gennisson, M. Tanter, and M. Fink, "Observation of shock transverse waves in elastic media," Phys. Rev. Lett. **91**, 164301 (2003).

[15] J. Ophir, I. Cspedes, H. Ponnekanti, Y. Yazdi, and X. Li, "Elastography: A quantitative method for imaging the elasticity of biological tissues," Ultrasonic Imaging **13**, 111–134 (1991), pMID: 1858217, https://doi.org/10.1177/016173469101300201.

[16] M. Tanter, J. Bercoff, L. Sandrin, and M. Fink, "Ultrafast compound imaging for 2-d motion vector estimation: application to transient elastography," IEEE Transactions on Ultrasonics, Ferroelectrics, and Frequency Control **49**, 1363–1374 (2002).

[17] D. Laskowitz and G. Grant, *Translational research in traumatic brain injury*, Vol. 57 (CRC Press, 2016).

[18] D. Espíndola, S. Lee, and G. Pinton, "Shear shock waves observed in the brain," Phys. Rev. Applied **8**, 044024 (2017).

[19] L. Zhang, K. H. Yang, and A. I. King, "Comparison of brain responses between frontal and lateral impacts by finite element modeling," Journal of neurotrauma **18**, 21–30 (2001).

[20] J. M. Buick, C. L. Buckley, C. A. Greated, and J. Gilbert, "Lattice boltzmann bgk simulation of nonlinear sound waves: the development of a shock front," Journal of Physics A: Mathematical and General **33**, 3917 (2000).

[21] G. Pinton, J. l. Gennisson, M. Tanter, and F. Coulouvrat, "Adaptive motion estimation of shear shock waves in soft solids and tissue with ultrasound," IEEE Transactions on Ultrasonics, Ferroelectrics, and Frequency Control **61**, 1489–1503 (2014).

[22] B. Giammarinaro, F. Coulouvrat, and G. Pinton, "Numerical simulation of focused shock shear waves in soft solids and a two-dimensional nonlinear homogeneous model of the brain," Journal of biomechanical engineering **138**, 041003 (2016).

[23] G. Pinton, F. Coulouvrat, J.-L. Gennisson, and M. Tanter, "Nonlinear reflection of shock shear waves in soft elastic media," The Journal of the Acoustical Society of America **127**, 683–691 (2010), https://doi.org/10.1121/1.3277202.

[24] M. F. Hamilton, Y. A. Ilinskii, and E. A. Zabolotskaya, "Separation of compressibility and shear deformation in the elastic energy density (l)," The Journal of the Acoustical Society of America **116**, 41–44 (2004), https://doi.org/10.1121/1.1736652.

[25] M. Destrade, G. Saccomandi, and M. Vianello, "Proper formulation of viscous dissipation for nonlinear waves in solids," The Journal of the Acoustical Society of America **133**, 1255–1259 (2013), https://doi.org/10.1121/1.4776178.

[26] J.-L. Gennisson, M. Rénier, S. Catheline, C. Barrière, J. Bercoff, M. Tanter, and M. Fink, "Acoustoelasticity in soft solids: Assessment of the nonlinear shear modulus with the acoustic radiation force," The Journal of the Acoustical Society of America **122**, 3211–3219 (2007), https://doi.org/10.1121/1.2793605.

[27] Y. Jiang, G. Li, L.-X. Qian, S. Liang, M. Destrade, and Y. Cao, "Measuring the linear and nonlinear elastic properties of brain tissue with shear waves and inverse analysis," Biomechanics and Modeling in Mechanobiology **14**, 1119–1128 (2015).

[28] M. Rénier, J.-L. Gennisson, C. Barrière, D. Royer, and M. Fink, "Fourth-order shear elastic constant assessment in quasi-incompressible soft solids," Applied Physics Letters **93**, 101912 (2008), https://doi.org/10.1063/1.2979875.

[29] B. E. McDonald and J. Ambrosiano, "High-order upwind flux correction methods for hyperbolic conservation laws," Journal of Computational Physics **56**, 448 – 460 (1984).

[30] J. A. TenCate, "An experimental investigation of the nonlinear pressure field produced by a plane circular piston," The Journal of the Acoustical Society of America **94**, 1084–1089 (1993), https://doi.org/10.1121/1.406955.